Evaluation of B_1 inhomogeneity effect on DCE-MRI data analysis of brain tumor patients at 3T

Anirban Sengupta[1], Rakesh Kumar Gupta[2] and Anup Singh[1,3,4*]

Abstract

Background: Dynamic-contrast-enhanced (DCE) MRI data acquired using gradient echo based sequences is affected by errors in flip angle (FA) due to transmit B_1 inhomogeneity (B_1inh). The purpose of the study was to evaluate the effect of B_1inh on quantitative analysis of DCE-MRI data of human brain tumor patients and to evaluate the clinical significance of B_1inh correction of perfusion parameters (PPs) on tumor grading.

Methods: An MRI study was conducted on 35 glioma patients at 3T. The patients had histologically confirmed glioma with 23 high-grade (HG) and 12 low-grade (LG). Data for B_1-mapping, T_1-mapping and DCE-MRI were acquired. Relative B_1 maps (B_{1rel}) were generated using the saturated-double-angle method. T_1-maps were computed using the variable flip-angle method. Post-processing was performed for conversion of signal–intensity time (S(t)) curve to concentration–time (C(t)) curve followed by tracer kinetic analysis (K^{trans}, Ve, Vp, Kep) and first pass analysis (CBV, CBF) using the general tracer-kinetic model. DCE-MRI data was analyzed without and with B_1inh correction and errors in PPs were computed. Receiver-operating-characteristic (ROC) analysis was performed on HG and LG patients. Simulations were carried out to understand the effect of B_1 inhomogeneity on DCE-MRI data analysis in a systematic way. S(t) curves mimicking those in tumor tissue, were generated and FA errors were introduced followed by error analysis of PPs. Dependence of FA-based errors on the concentration of contrast agent and on the duration of DCE-MRI data was also studied. Simulations were also done to obtain K^{trans} of glioma patients at different B_{1rel} values and see whether grading is affected or not.

Results: Current study shows that B_{1rel} value higher than nominal results in an overestimation of C(t) curves as well as derived PPs and vice versa. Moreover, at same B_{1rel} values, errors were large for larger values of C(t). Simulation results showed that grade of patients can change because of B_1inh.

Conclusions: B_1inh in the human brain at 3T-MRI can introduce substantial errors in PPs derived from DCE-MRI data that might affect the accuracy of tumor grading, particularly for border zone cases. These errors can be mitigated using B_1inh correction during DCE-MRI data analysis.

Keywords: DCE-MRI, B_1 inhomogeneity, Flip-angle errors, Glioma grading, Brain-tumor

Background

Dynamic contrast-enhanced (DCE) MRI [1] is widely used for characterization and diagnosis of intracranial mass lesions [2]. A number of studies have shown the potential of DCE-MRI in diagnosis and treatment of brain tumor [3–6]. DCE-MRI has been in clinical and pre-clinical practice for more than two decades. Various mathematical models exist for analyzing DCE-MRI data [1, 7–13]. Using the General Tracer Kinetic Model (GTKM) model [1], DCE-MRI data can be used for extraction of various parameters viz. tracer kinetic parameters like volume transfer rate (K^{trans}), volume of extravascular extracellular space (Ve), plasma volume

*Correspondence: anups.minhas@gmail.com; anupsm@iitd.ac.in
[4] Centre for Biomedical Engineering, IIT Delhi, Block-II, Room No. 299, Hauz Khas, New Delhi 110016, India
Full list of author information is available at the end of the article

Sengupta *et al. J Transl Med* (2017) 15:242

Page 2 of 13

(Vp), as well as first pass analysis parameters like cerebral blood volume (CBV) and cerebral blood flow (CBF).

In general, DCE MRI data is acquired using fast Gradient Recalled Echo (GRE) sequences like SPGR/TFE. This makes the signal intensity of DCE-MRI dependent upon FA. MRI images which are acquired using gradient echo based sequences are sensitive to B_1 inhomogeneity at high field MRI scanner like 3T [14] up to 9T [15] depending upon RF coil and type of tissue used. This field inhomogeneity introduces flip angle (FA) related errors in signal intensity. Moreover, the FA errors can propagate to further quantitative analysis.

In a previously reported study [16] on breast tissue and simulated data, propagation of FA errors in DCE-MRI data was investigated and it was reported that errors in K^{trans} and Ve vary non-linearly with FA. Propagations of FA related errors to enhancement ratio, relative change between pre and post contrast, was previously reported for breast tissue [17]. Recently, another study on the effect of transmit B_1 inhomogeneity on tracer kinetic analysis of DCE-MRI data from breast cancer patients was also reported [18]. In this study effect of B_1 inhomogeneity on pre-contrast T_1 and kinetic parameters (K^{trans} and Ve) were reported. Propagations of FA-based errors on AIF estimations has also been reported for prostate tissue at 3T [19]. Thus there is a need for a systematic study using simulations and in vivo data, for evaluating propagation of errors on computed concentration and various perfusion parameters in the human brain.

Measurement of the T_1 parameter is a pre-requisite for DCE-MRI analysis. A number of methods based upon inversion recovery [20, 21], Look locker [22], MOLLI [23], multiple Fast Spin Echo (FSE) image [24], and multiple FA [25, 26] are available for T_1 estimation. T_1 estimation based upon multiple FA is widely used due to shorter data acquisition time. However, T_1 estimation using multiple FA based methods are sensitive to B_1 field inhomogeneity [27–29]. In such cases, correction of T_1 maps for B_1 inhomogeneity is performed before further DCE MRI data analysis [30–34].

In the current study, in vivo DCE-MRI data and B_1 field map data from human brain tumor patients were acquired at 3T MRI to evaluate the effect of B_1 inhomogeneity at different stages of DCE-MRI analysis. Corrections for B_1 inhomogeneity were applied during DCE-MRI signal to concentration conversion. In addition, T_1 map data was also acquired using multiple flip angles and corrected for B_1 inhomogeneity. Simulations were performed to evaluate systematically the propagation of FA errors on DCE-MRI data analysis. The clinical significance of B_1 inhomogeneity was also investigated using statistical analysis and simulation studies.

Methods

Study population

The study protocol was pre-approved by the Institutional Review Board of the Institute and all subjects provided written informed consent before MR scanning. The IRB Approval Number for this study is 2013-001IP-05. Thirty-five patients (Male = 25, Female = 10) having a mean age of 50.54 ± 15.36 years (age range 16–77 years) were recruited for the study. The patients had histologically confirmed glioma with 23 high grade (HG) [21 Grade IV and 2 Grade III] and 12 low grade (LG) [11 Grade II and 1 Grade I]. Grading was done as per World Health Organization guidelines.

MRI measurements

All MRI experiments were performed at 3T whole-body MRI system (Ingenia, Philips Healthcare, The Netherlands) using a 16 channel receive only coil. In this study, Multi Transmit parallel RF transmission was used to acquire MRI data. MRI protocol for this study included a tri-plane localizer acquiring conventional images for brain tumor patient, data for T_1 maps, data for B_1 maps and DCE-MRI data.

For T_1 mapping, 3D T_1W Turbo field echo (TFE) images were acquired with four FAs of 3°, 6°, 10° and 15°. Twelve slices, covering the tumor part, were acquired. Other MRI scan parameters were: slice thickness = 6 mm; FOV = 240×240 mm^2; matrix size = 256×256; TR/TE of 6.0/2.1 ms.

MRI data for B_1 map was also collected for all the subjects. Saturated dual angle method [30], with two FA interleaved approach, was used for B_1 mapping. 2D TSE readout was used to acquire saturated dual angle images corresponding to 60° and 120°. FOV and number of slices were same as used in T_1W TFE images. TR/TE of 600/40 ms was used to acquire images.

In the final step, DCE perfusion imaging was performed using a T_1 Turbo field echo sequence (TR/TE = 4.45/2.01 ms; FA = 10; slice thickness = 6 mm; FOV = 240×240 mm^2; matrix size = 256×256). At the fourth time point of the 3D-DCE-MRI data acquisition, 0.1 mmol/kg body weight of gadobenate dimeglumine Gd-BOPTA (Multihance, Bracco) was administered intravenously with the help of a power injector at a rate of 3.0 ml/s, followed by a bolus injection of a 30-ml saline flush [11]. A series of 384 images, 32 time points for 12 slices, were acquired with a temporal resolution of 3.9 s.

Quantification of perfusion parameters

In the current study, DCE-MRI data analysis involved following steps:

Sengupta *et al. J Transl Med* (2017) 15:242

Page 3 of 13

B_1 mapping

The B_1 map was generated using saturated double angle based method [30]. Two images are acquired: I1 and I2 such that the tip angle of I2 is twice of I1. All other signal-affecting sequence parameters are kept constant. If the effects of T_1 and T_2 relaxation can be neglected, then it can be shown that

$$\theta = \cos^{-1}\left(\frac{I_2}{2 \cdot I_1}\right) \tag{1}$$

Here θ corresponds to the tip angle that vary with the spatially varying B_1 field. I_1 and I_2 corresponds to images obtained at FA 60° and 120° respectively. Computed angle θ was divided by angle of 60° degree to generate relative B_1 (B_{1rel}) map. True or nominal value corresponds to $B_{1rel} = 1$.

Mean ($\pm$SD) value of B_{1rel} map for all slices of 35 patients were computed and plotted. This has been done on both entire brain region covering all slices and on entire tumor region of a particular slice to estimate the B_1 inhomogeneity range among these patients.

Estimation of T_1

T_1 map was computed using previously reported multiple FA based method [35]. The FAs used in the current study were 3°, 6°, 10° and 15°. T_1 maps using multiple FA based method were generated by fitting the pixel-wise image intensities of the above-mentioned FAs to Eq. (2) (described in the next section) using a non-linear least-square fitting routine in MATLAB. The 'lsqcurvefit' routine in MATLAB with lower and upper bound of 200 and 5000 ms and an initial guess of 1000 ms was used for curve fitting. The lsqcurvefit routine uses the trust-region-reflective algorithm. For obtaining B_1 inhomogeneity corrected T_1 map, all FAs were corrected pixel-wise for B_1 inhomogeneity using B_{1rel} map [30].

Effect of B_1 inhomogeneity on DCE-MRI data and its corrections

Signal intensity for SPGR/TFE signal is represented by the following equation:

$$S = \frac{M_0 \cdot \sin(\theta) \cdot e^{-\frac{TE}{T_2^*}} \cdot \left(1 - e^{-\frac{TR}{T_1}}\right)}{1 - \cos(\theta) \cdot e^{-\frac{TR}{T_1}}} \tag{2}$$

where M_0 is the equilibrium longitudinal magnetization. M_0 is given as $G \cdot \rho$ where G is the gain and ρ is the proton density. TR and TE represents repetition and echo times, T_1 and T_2^* are relaxation times and θ is the FA.

The signal S is a function of θ. Therefore, DCE MRI data which is acquired before, during and after intravenous injection of contrast agent show dependence on FA. B_1 field inhomogeneity results in variation of nominal FA and hence in the signal intensity time curve (S(t)) of DCE-MRI data. These variations propagate to further DCE-MRI analysis. Due to B_1 inhomogeneity, voxelwise FA (at ith voxel) is given by the following equation:

$$\theta(i) = \theta_{nominal} \cdot B_{1rel}(i) \tag{3}$$

Here $\theta(i)$ is the modified FA at ith voxel, according to B_{1rel} value at corresponding voxel, and $\theta_{nominal}$ is the nominal value specified by user in MRI protocol. Since, data provided by scanner at a voxel (i) correspond to $\theta(i)$ given by Eq. (3) therefore, during quantitative analysis, $\theta(i)$ should be used instead of $\theta_{nominal}$ in order to remove the effect of B_1 field inhomogeneity.

Since we are mainly interested in quantitative analysis of DCE-MRI data and the first step is the conversion of S(t) toC(t), therefore, it's important to correct C(t) for B_1 inhomogeneity. In this study, S(t) was converted to C(t) using previously described procedure [24].

Contrast agent changes the relaxation rates of tissues. The increase in relaxation rates are linearly related to contrast concentration in the tissue:

$$\frac{1}{T_1^*} = \frac{1}{T_{10}} + r1 \cdot C(t) \quad \text{and} \quad \frac{1}{T_2^*} = \frac{1}{T_{20}} + r2 \cdot C(t) \tag{4}$$

Here r1 = 5.9 l/mmol/s and r2 = 17.5 l/mmol/s at 37 °C and 3T [36]. After injection of contrast, the signal from an SPGR sequence is given by [24]:

$$S(t) = G \cdot \rho \cdot \exp\left(-TE \cdot (T_{20}^{-1} + r2 \cdot C(t))\right) \cdot \sin(\theta) \cdot \\ \frac{1 - \exp\left(-TR\,(T_{10}^{-1} + r1 \cdot C(t))\right)}{1 - \cos(\theta) \cdot \exp\left(-TR\,(T_{10}^{-1} + r1 \cdot C(t))\right)} \tag{5}$$

For this particular study, TE is small enough to neglect its effect. Briefly, the above equation can be reduced to

$$\frac{S(t)}{S(0)} = \frac{K_0 \cdot E2 \cdot (1 - E3)}{1 - \cos(\theta) \cdot E3} \tag{6}$$

where $K_0 = (1 - \cos(\theta) \cdot e^{(-TR/T_{10})}) / (1 - e^{(-TR/T_{10})})$, $E3 = e^{\left(-TR \cdot \left(\frac{1}{T_{10}} + r1 \cdot C(t)\right)\right)}$.

T_{10} is the value of T_1 of tissues before injection of contrast agent. C(t) is the concentration of Gd-BOPTA at time 't' in the tissue and C(0) = 0. Since in this study, T_{10} is estimated separately, therefore, Eq. (6) is a non-linear equation with only 1 unknown parameter C(t). This equation was solved to obtain the value of C(t) at different time points.

While converting S(t) to C(t), voxelwise FA as given by Eq. (3) was used. Here only pre-contrast T_1 values (T_{10}) are required as opposed to $T_1(t)$ at each time point

Sengupta *et al. J Transl Med* (2017) 15:242

Page 4 of 13

during direct correction of S(t). This step resulted in B_1 inhomogeneity corrected C(t) curves. For generating C(t) without B_1 inhomogeneity correction, we used $\theta_{nominal}$ as the θ in Eq. (6).

Estimation of AIF
In this study, we have used automatically detected local arterial input function (AIF) for each glioma patient using previously described procedure [10]. Briefly, the method for automatic extraction of AIF is based on the features exhibited by the concentration–time curve in vascular voxels. The main features of concentration–time curve at arterial voxels are: early arrival of contrast or early bolus arrival time, high peak value (during first pass), early arrival of time to peak; sharp uptake (high gradient value) of contrast agent, and high average value of concentration of contrast.

Tracer kinetic model fitting
In the current study we have used generalized tracer kinetic model (GTKM) described previously [1] for estimating kinetic parameters particularly volume transfer rate (K^{trans}), volume of extracellular extravascular space (Ve), plasma volume (Vp) and Kep which is the ratio of K^{trans} and Ve. Briefly, following equation of GTKM is used:

$$C_T(t) = V_p C_p(t) + K^{trans} \int_0^t C_p(\tau) e^{Kep(\tau - t)} d\tau \quad (7)$$

where C_T is the concentration of contrast in tissue/voxel and Cp is AIF. Voxel-wise fitting of GTKM was performed using in-house written programs in MATLAB and inbuilt MATLAB routine function 'lsqcurvefit' which uses the trust-region-reflective algorithm. The upper bound and lower bound values for K^{trans}, Kep and Vp was [1, 2, 8] and [0, 0, 0]. Ve was estimated as the ratio of K^{trans} and Kep. Tracer kinetic model fitting followed the previously described procedure [24].

First pass analysis
First pass analysis [37] for estimation of hemodynamic maps of CBF, CBV and corrected CBV (CBV_Corr) were carried out using previously described procedure [24]. It needs to be mentioned here that there is an overestimation of CBV in the regions where the contrast leaks into extravascular extracellular space because in this case, it represents the volume of contrast in intravascular as well

as in leakage space. CBV_Corr represents the volume of blood only in the intravascular space and is to be estimated by removing the contribution of fractional leakage space volume (Ve) from the CBV.

Sample size estimation
To evaluate the clinical significance of B_1 inhomogeneity statistical analysis was performed. The sensitivity and specificity of the perfusion parameters were calculated using receiver-operating characteristic (ROC) analysis. To estimate the sample size required for differentiation between HG and LG patients, it was assumed that the area under the ROC curve (AUC) of 0.8 is significant from the null hypothesis value 0.5 (meaning no discriminating power). For 95% power and a 0.1 level of significance, the minimum sample size required for positive (HG) and negative responses (LG) was 22 and 11 respectively. A total of 23 high grade (HG) which is Grade-4 and Grade-3 combined and 12 low grade (LG) which is Grade-2 and Grade-1 combined, patients were taken for this study.

Statistical analysis
Within the tumor region of a particular slice, 2–3 circular regions of 5 voxel radius showing high values of post B_1 corrected CBV_Corr were manually placed and the one showing maximum value was chosen as Region of Interest (ROI). All perfusion parameters before B_1 correction and after B_1 correction were obtained from the ROIs. Relative percentage error (RPE) for with and without B_1 inhomogeneity correction, were computed for C(t) and perfusion parameters corresponding to these ROIs. RPE was defined as:

$$RPE = \frac{(\text{Observation before correction} - \text{ observation after correction})}{\text{Observation after correction}} \times 100$$

These perfusion parameters were further used for ROC analysis. Cutoff value at which the average of sensitivity and specificity is maximized and area under the curve of ROC analysis were obtained for grading between HG and LG gliomas. Histologically confirmed grades were taken as a gold standard. All analysis was done using SPSS statistics software package version 16.0. A paired t test with two-tailed distribution was done to find out whether the change in each perfusion parameter before and after B_1 correction is significant or not. The Bland–Altman (BA) plot was also computed to compare values of perfusion parameters before and after B_1 correction.

Sengupta *et al. J Transl Med* (2017) 15:242

Page 5 of 13

In this graphical method, the differences between the two techniques are plotted against the averages of the two techniques. Here the difference of parameters is plotted against post-B_1 correction technique since that is the reference method. The mean difference should be less than the limits of agreement which is defined as the 95% CI of the mean difference, for the agreement between results of with and without correction.

Simulations

Simulations were carried out to understand the effect of B_1 inhomogeneity on DCE-MRI data analysis in a systematic way. Equation (6) was used for simulating S(t) curves mimicking those in tumor tissues. Parameters used in the simulation are shown in Table 1. For simulated AIF we have used parameters as reported in the literature [38]. Three cases were simulated in this study. In the 1st case, C(t) values from 0:0.01:0.5 mmol/l were used to generate S(t) curve using Eq. (6). Now while converting back from S(t) to C(t), errors in FA were introduced for mimicking B_1 field inhomogeneity effect. This was done to understand the effect of initial concentration amount

Table 1 Parameters used in simulations

Parameters	Values
T_{10}	1500 ms
TR	4.45 ms
Flip angle (FA)	10
r1	5.9 l/mmol/s
r2	17.5 l/mmol/s
Scaling factor	1000
Time points	32
B1 inhomogeneity	0.8–1.2 at step size of 0.05
$[K_{ep}, V_p]$ at staring point	[0.5, 0.02]

on an error in C(t) due to different B_1 inhomogeneity errors. In the 2nd case, C(t) curves mimicking response of tumor tissue were generated without and with different B_1 inhomogeneity errors. This was done to evaluate the error in C(t) due to B_1 inhomogeneity. In 3rd case, three C(t) curves having different concentration amounts (mimicking those in tumor tissue) were generated and effect of B_1 inhomogeneity errors in various parameters were computed. This involved using different K^{trans} values [0.1, 0.2, 0.3] as the starting values to generate three different C(t) while keeping Kep and Vp values fixed as shown in Table 1. The goal of this study was to estimate the change in perfusion parameters as a result of change in C(t) curves due to FA error. It needs to be mentioned that in simulation studies the FA for dynamic study is 10° which is same as the FA used in in vivo data.

Another simulation study was done to illustrate the clinical significance of B_1 inhomogeneity correction. 5 HG (Grade3 and Grade-4) and 5 LG (Grade-1 and Grade-2) patients were randomly selected. K^{trans} values after B_1 correction corresponding to the chosen ROI were used. B_{1rel} was altered from a range of 0.75–1.25 to see how it influences the perfusion parameters. The C(t) values were kept same for all of them to study the influence of B_1 exclusively on perfusion parameters. The threshold for grading used in this study was same as that obtained from ROC analysis after B_1 correction.

Results

In the current study, it was evident that B_1 inhomogeneity was present across different MRI image slices of human brain. Figure 1 shows B_{1rel} maps of multiple brain slices of one subject. B_{1rel} values were higher than the nominal value of 1 in the central part of the brain. In the
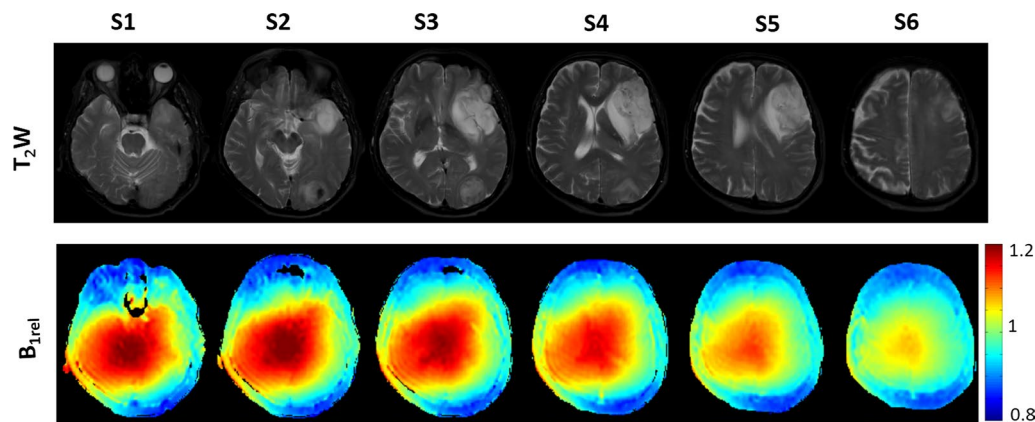

Fig. 1 Shows T_2W images (1st row) and B_{1rel} maps (2nd row) from six alternate slices of a human brain tumor patient. Voxels with B_{1rel} value of 1 corresponds to the nominal B_{1rel} value

Sengupta *et al. J Transl Med (2017) 15:242*

Page 6 of 13

peripheral region of the brain, B_{1rel} values are found to be less than the nominal value of 1.

Histogram plot of B_{1rel} values for 12 brain slices of a particular patient in Fig. 2a shows a broad distribution of B_{1rel} values which extends to both sides of the nominal value. For this subject, B_{1rel} values range in the brain slices were [0.85–1.25] with the maximum value found between 1 and 1.05. Figure 2b, c show plots of B_{1rel} values (mean $\pm$ SD) of the entire brain and tumor tissue respectively for 35 different subjects. Large variations in B_{1rel}

values of entire brain was observed in each of 35 patients. More importantly, it was observed that mean B_{1rel} values ranged from 3% below nominal to 20% above nominal in the tumor region among different patients.

Table 2 shows B_{1rel} values and corresponding relative percentage error (average value $\pm$ S.D) of different parameters at the previously mentioned ROI in tumor region for 35 different patients. B_{1rel} values ranging from 0.95 to 1.25 at an interval of 0.05 has been shown. RPE of all perfusion parameters shows an increasing trend
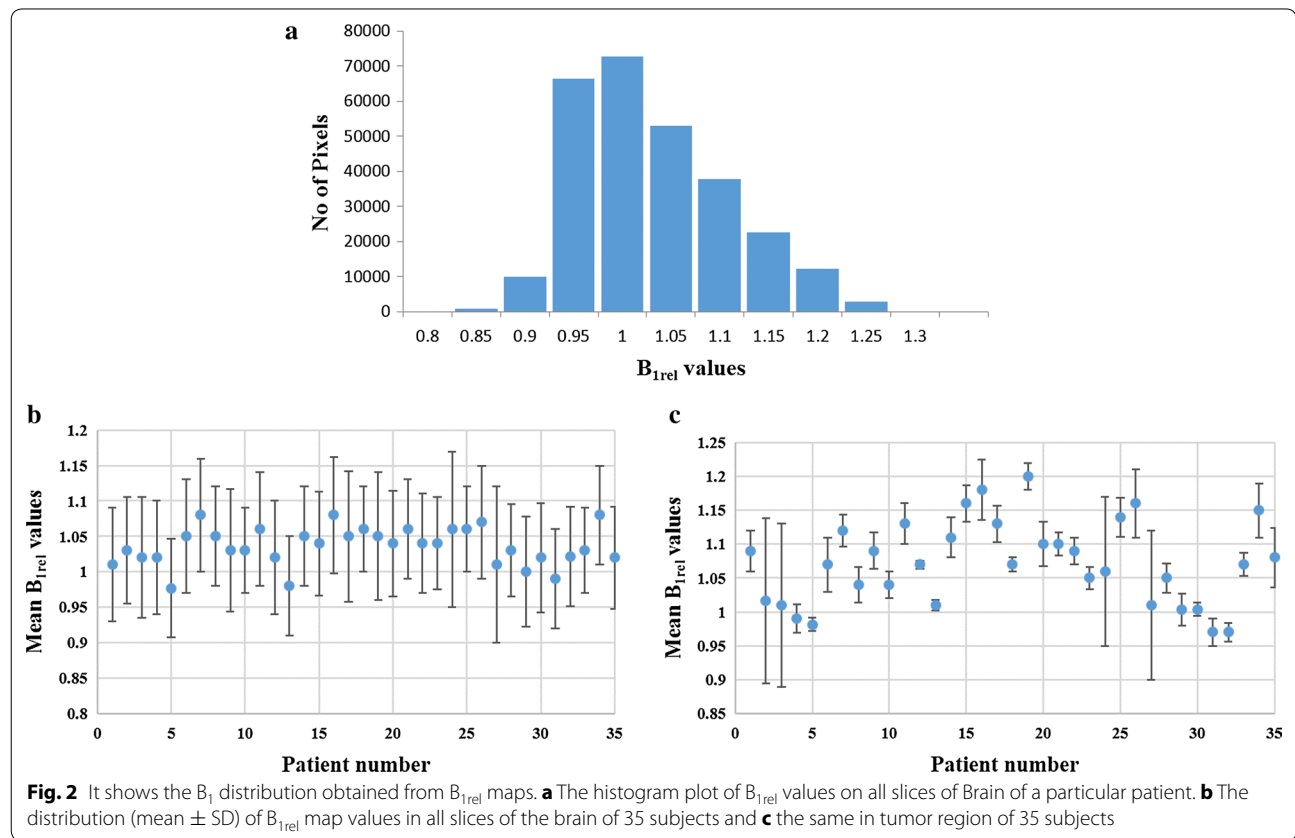

Fig. 2 It shows the B_1 distribution obtained from B_{1rel} maps. **a** The histogram plot of B_{1rel} values on all slices of Brain of a particular patient. **b** The distribution (mean $\pm$ SD) of B_{1rel} map values in all slices of the brain of 35 subjects and **c** the same in tumor region of 35 subjects

Table 2 Relative percentage error (RPE) in parameters, derived from DCE-MRI data analysis

B1	Relative % error (mean $\pm$ S.D)					
	K^{trans}	Ve	Vp	CBV	CBF	CBV_Corr
0.95–1	-0.85 ± 0.70	-0.96 ± 0.87	-0.42 ± 1.33	-1.02 ± 0.794	-1.22 ± 0.786	-0.84 ± 0.815
1–1.05	0.26 ± 1.80	9.10 ± 17.99	1.25 ± 0.80	1.28 ± 0.50	1.17 ± 0.408	1.66 ± 1.91
1.05–1.10	3.77 ± 1.19	5.50 ± 2.80	3.03 ± 1.65	3.49 ± 0.95	3.27 ± 1.47	2.75 ± 0.76
1.10–1.15	5.62 ± 2.52	19.12 ± 13.10	6.64 ± 3.41	6.01 ± 1.79	6.44 ± 2.48	4.19 ± 1.23
1.15–1.20	9.74 ± 2.44	14.78 ± 9.84	7.22 ± 1.70	8.48 ± 0.92	9.49 ± 3.63	7.12 ± 1.28
1.20–1.25*	12.91	12.86	9.70	10.51	10.52	9.69

RPE of each parameter from brain tumor of 35 patients were grouped based upon range of $B1_{rel}$ value
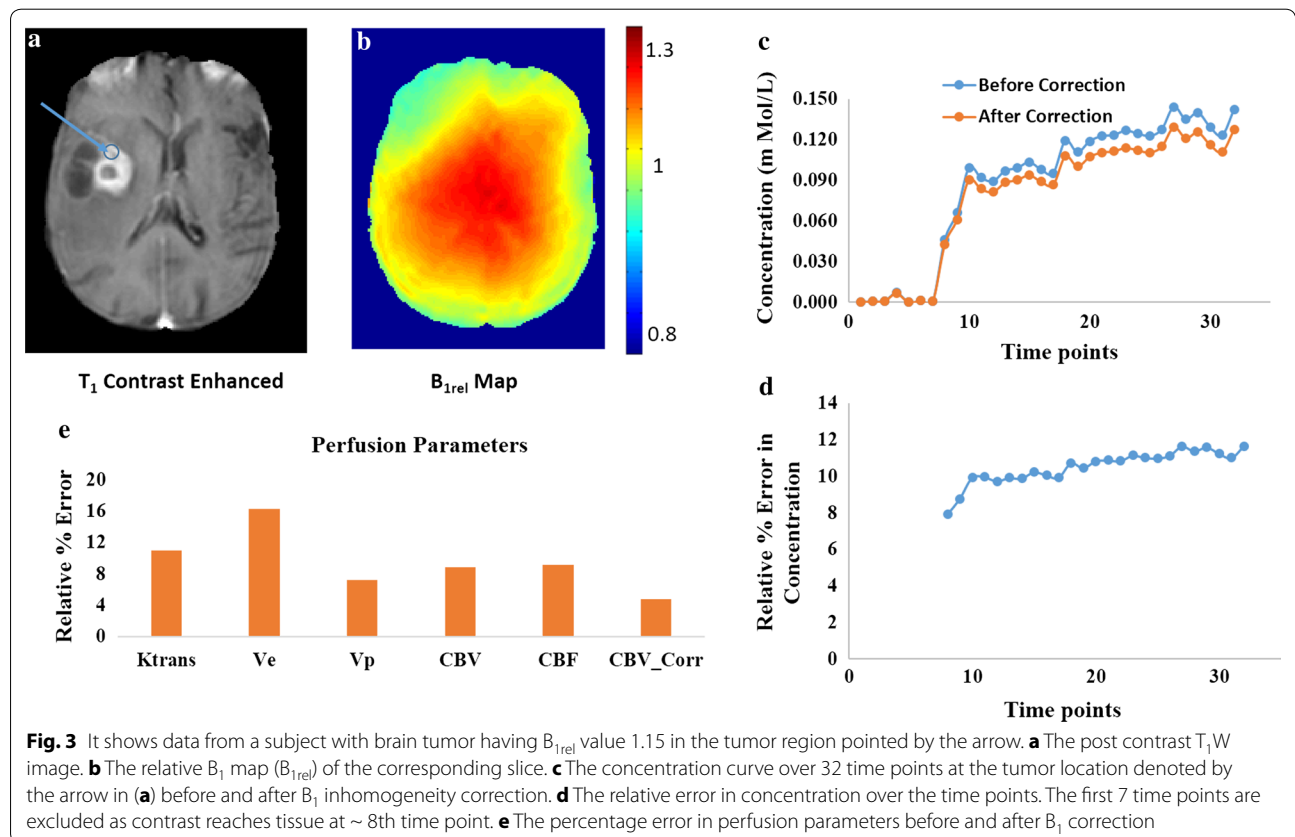
* This group had only one patient and hence no S.D

Sengupta *et al. J Transl Med* (2017) 15:242

Page 7 of 13

with an increase of B_{1rel} values. For B_{1rel} values less than the nominal range (which is equal to 1), RPE of perfusion parameters is negative and vice versa. Kep's values are not presented in the table as it is not an independent parameter, being the ratio of K^{trans} and Ve.

Figure 3 show data from a patient with glioblastoma (GBM) having a B_{1rel} value of 1.15 in an ROI in the tumor region pointed by the arrow. An enhancing ring like tumor region is visible in that slice. In the ROI a steep rise in concentration was observed because of contrast leakage into the tumor due to the Blood Brain Barrier breakdown. In Fig. 3b B_{1rel} map shows the inhomogeneous B_1 distribution in the particular slice of brain. Figure 3c shows that C(t) at the tumor location reduces after B_1 inhomogeneity correction over 32 time points. Figure 3d shows that there is a relative percentage error of 11.65% in concentration at the end of 32 time points. Bolus arrival time for this ROI was at the 8th time point. Therefore, first 7 time points were excluded from error computation. Figure 3e shows the relative percentage error in various perfusion parameters due to B_1 inhomogeneity. It shows that a B_{1rel} value greater than nominal value (before correction) results in an overestimation of parameters CBV, CBV-Corr, CBF, K^{trans}, Ve, Vp. For this subject, Ve showed maximum RPE of $\sim$ 16%.

Figure 4 shows data from a subject with brain tumor having a B_{1rel} value of 0.94 (lower than nominal value) in the tumor region. Figure 4a shows the tumor location in the post-contrast T_1W image. Figure 4b shows that the B_{1rel} value in the ROI taken from tumor region is below the nominal value. Figure 4c shows the C(t) at the tumor ROI is increased after B_1 Correction. Figure 4d shows that there is a relative percentage error of 6.3% in concentration at the end of 32 time points. Bolus arrival time for this ROI was around 9th time point. Therefore, first 8 time points were excluded from error computation. The lower value of B_{1rel} results in an underestimation of C(t), which was corrected after B_1 inhomogeneity correction. Similarly, all perfusion parameters, show underestimation with a relative percentage error of K^{trans} reaching $-$ 6.3% shown by in Fig. 4e.

Table 3 gives relative % change in variation (calculated as square of SD) of each perfusion parameter for both HG and LG patients. Mostly, it was seen that variation of perfusion parameters reduced after correction within each grade.

Dependence of FA related errors, using simulations, in computed concentration on the amount of nominal concentration is shown in Fig. 5. It was observed that FA related errors increase with an increase in the amount of concentration. Figure 6 show propagation of B_{1rel}
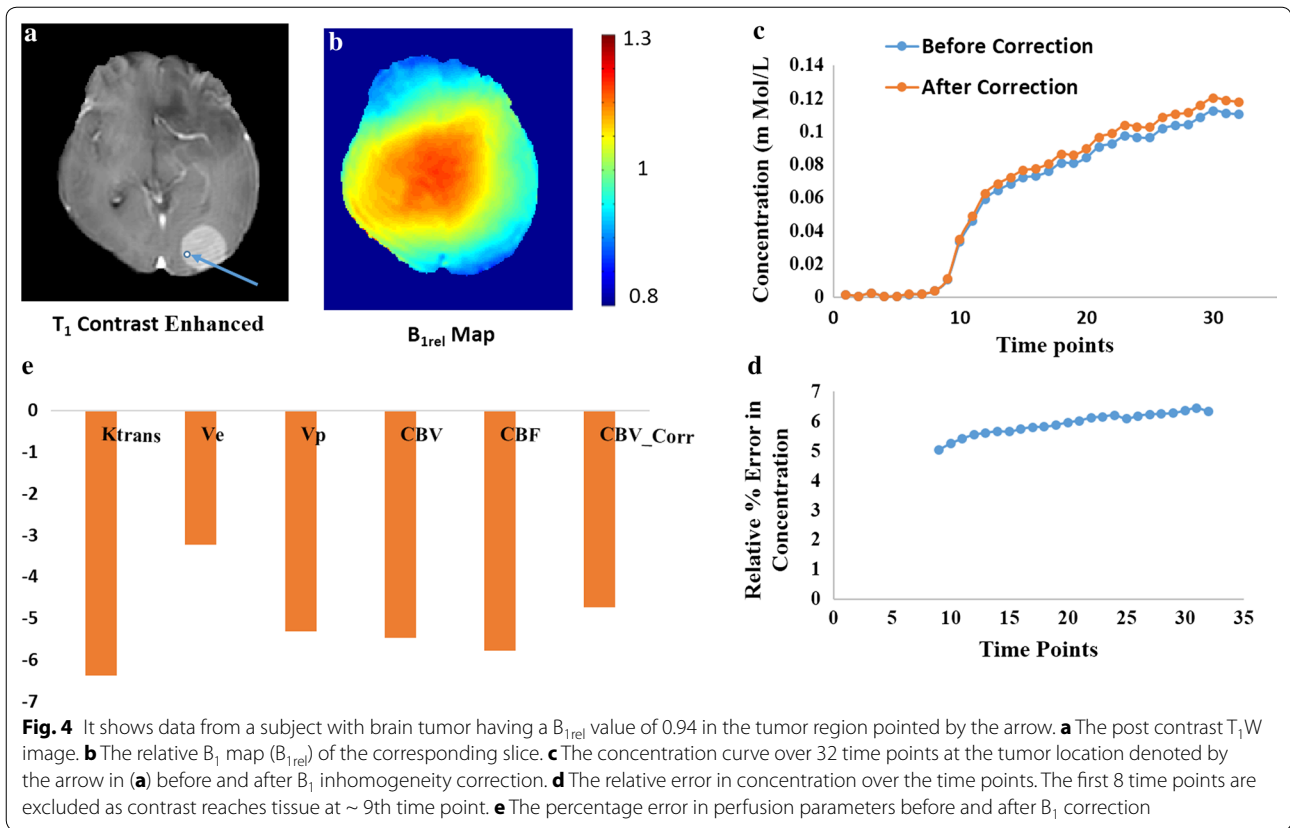

Fig. 3 It shows data from a subject with brain tumor having B_{1rel} value 1.15 in the tumor region pointed by the arrow. **a** The post contrast T_1W image. **b** The relative B_1 map (B_{1rel}) of the corresponding slice. **c** The concentration curve over 32 time points at the tumor location denoted by the arrow in (**a**) before and after B_1 inhomogeneity correction. **d** The relative error in concentration over the time points. The first 7 time points are excluded as contrast reaches tissue at $\sim$ 8th time point. **e** The percentage error in perfusion parameters before and after B_1 correction

Sengupta *et al. J Transl Med* (2017) 15:242

Page 8 of 13

Fig. 4 It shows data from a subject with brain tumor having a B_{1rel} value of 0.94 in the tumor region pointed by the arrow. **a** The post contrast T_1W image. **b** The relative B_1 map (B_{1rel}) of the corresponding slice. **c** The concentration curve over 32 time points at the tumor location denoted by the arrow in (**a**) before and after B_1 inhomogeneity correction. **d** The relative error in concentration over the time points. The first 8 time points are excluded as contrast reaches tissue at ~ 9th time point. **e** The percentage error in perfusion parameters before and after B_1 correction

Table 3 Relative % change in variation of perfusion parameters within high and low grade patients

Parameters	High grade	Low grade
K^{trans}	6.605796	15.10635
Ve	6.638113	15.83864
Vp	15.21406	1.00593
CBV	6.233672	7.027053
CBF	4.495963	− 0.80946
CBV_Corr	9.547645	6.775655

Relative % change = 100 × (variation before correction − variation after correction)/variation after correction

errors to simulated C(t). Simulated C(t) curve mimics those of contrast enhancing tumor region. Simulations show that values of B_{1rel} lower than nominal value results in an underestimation of C(t) while higher values result in overestimation. This behavior was similar to experimental results obtained from brain tumor patients.
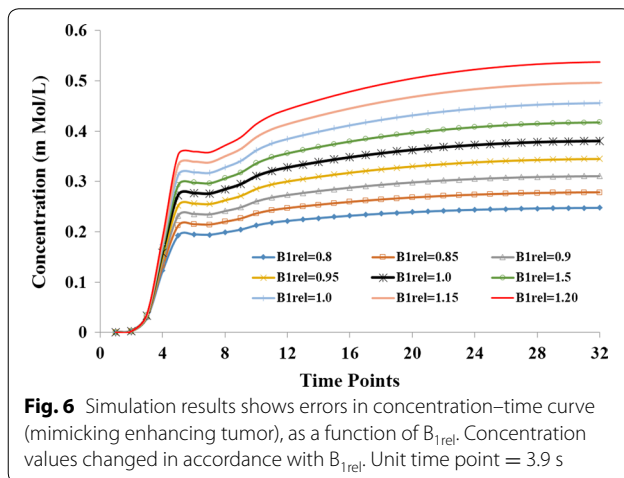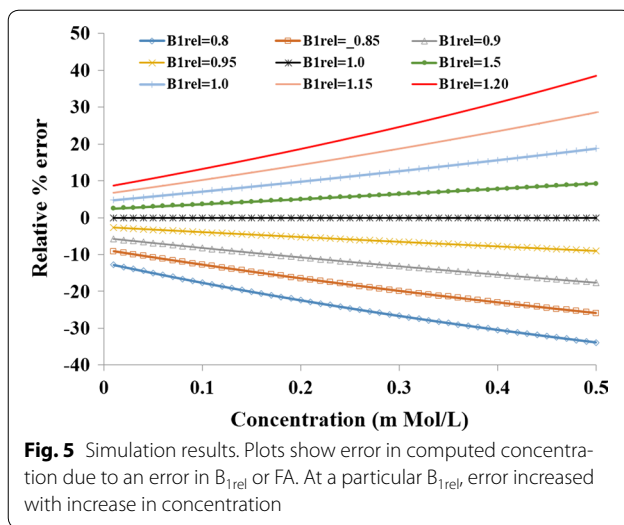
Simulation results shown in Fig. 7 demonstrate the dependence of B_1 inhomogeneity related errors in perfusion parameters on the concentration of contrast agent. Overall, errors in all the parameters increased with increase in the concentration of contrast agent. Parameter Ve showed the maximum error.

Figure 8a shows that the cut-off for K^{trans} between HG and LG patients is 0.77. Patient 2, 8, 10 were HG and remained HG at different B_{1rel} values. Patient 1, 5, 7 were LG and remained LG with a change in B_{1rel} values. Patient 4 changed from HG to LG at B_{1rel} less than 8, patient 3 changed from HG to LG at a B_1 value less than 0.95, patient 6 changed from LG to HG at B_{1rel} greater than 1.15 whereas patient 9's grade changed from LG to HG at the B_{1rel} value of 1.25 or more. Figure 8b shows the same graph for borderline patients 3, 4, 6 and 9 for better visualization.

Paired t test result showed that changes in each perfusion parameter before and after correction is significantly different (p < 0.001). In Fig. 9 Bland–Altman plots for perfusion parameters showed that for each parameter the mean difference fell within the limits of agreement for the majority of subjects. However, for all metrics, two to three subjects fell outside the limits of CI.

Discussion

In the current study, B_1 inhomogeneity in the human brain with tumor at 3T MRI was estimated and its effect on concentration–time curves and derived perfusion parameters was evaluated using experimental as well as simulated data. Mean B_{1rel} ranged from 3% below

Sengupta *et al. J Transl Med* (2017) 15:242

Page 9 of 13

Fig. 5 Simulation results. Plots show error in computed concentration due to an error in B_{1rel} or FA. At a particular B_{1rel}, error increased with increase in concentration

Fig. 6 Simulation results shows errors in concentration–time curve (mimicking enhancing tumor), as a function of B_{1rel}. Concentration values changed in accordance with B_{1rel}. Unit time point = 3.9 s

nominal to 20% above nominal in tumor tissues of different patients, which resulted in erroneous estimates of concentrations as well as perfusion parameters. It was also observed that B_{1rel} in tumor ROI is lower than nominal for few patients whereas it was higher than nominal for the majority of patients. This resulted from the heterogeneous B_{1rel} field across the brain. Centre of the brain shows B_{1rel} values much higher than nominal compared to the periphery. Thus tumor near the central part of the brain had higher B_{1rel} values compared to a tumor in the periphery region. Simulation results provided a systematic evaluation of propagation of FA related errors in DCE-MRI data analysis. The current study shows that B_{1rel} value greater than nominal results in overestimation of C(t) curves as well as derived perfusion parameters. Similarly, B_{1rel} values lower than nominal result in underestimation of parameters. Kep being a ratio of K^{trans} and Ve didn't provide any unique information and hence was

not mentioned in the results. Preliminary results of this study have been reported [39].

One of the observations in the current study was that errors in C(t) due to B_1 inhomogeneity increases non linearly with increase in concentration amount. The amount of concentration in contrast enhancing tumor region is different for different patients. The errors in perfusion parameters have a complex dependence on the amount of concentration and B_{1rel} value at a particular ROI.

In the current study, a 2D TSE readout technique was used to acquire B_1 map data. This technique is intrinsical to slice selection because of slice selective refocusing pulses. So, a non-selective excitation pulse (at 2 different angles) can be used without having to go for a 3D volume acquisition. Thus the used sequence provides fast and accurate results without taking into account the slice profile of excitation pulse. Moreover, during dynamic image acquisition, an echo time of 2.1 ms was used. It was seen through some preliminary studies that changes in T_{20} at such a small TE didn't affect the calculation of DCE parameters. Thus in this study, we have neglected the effect of T_{20}.
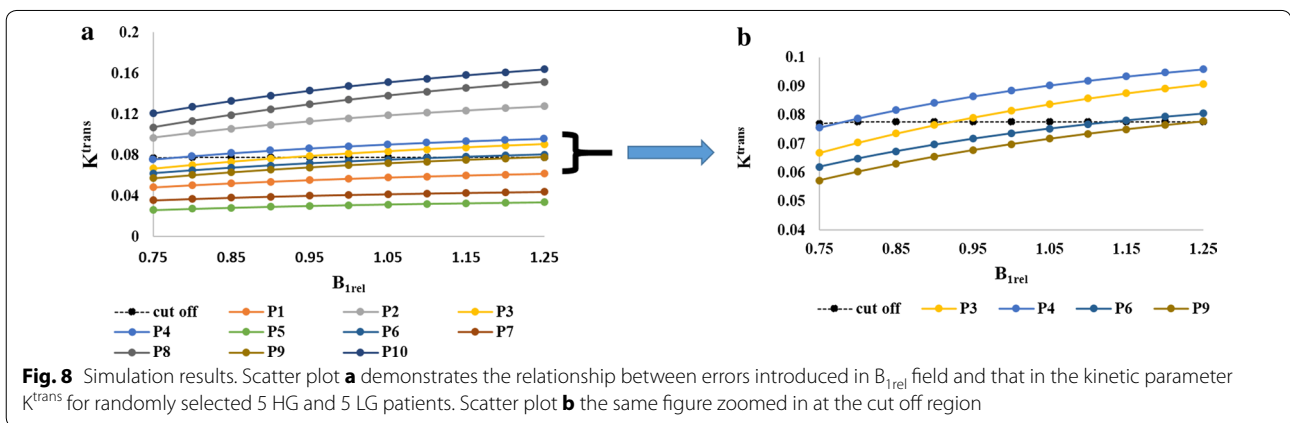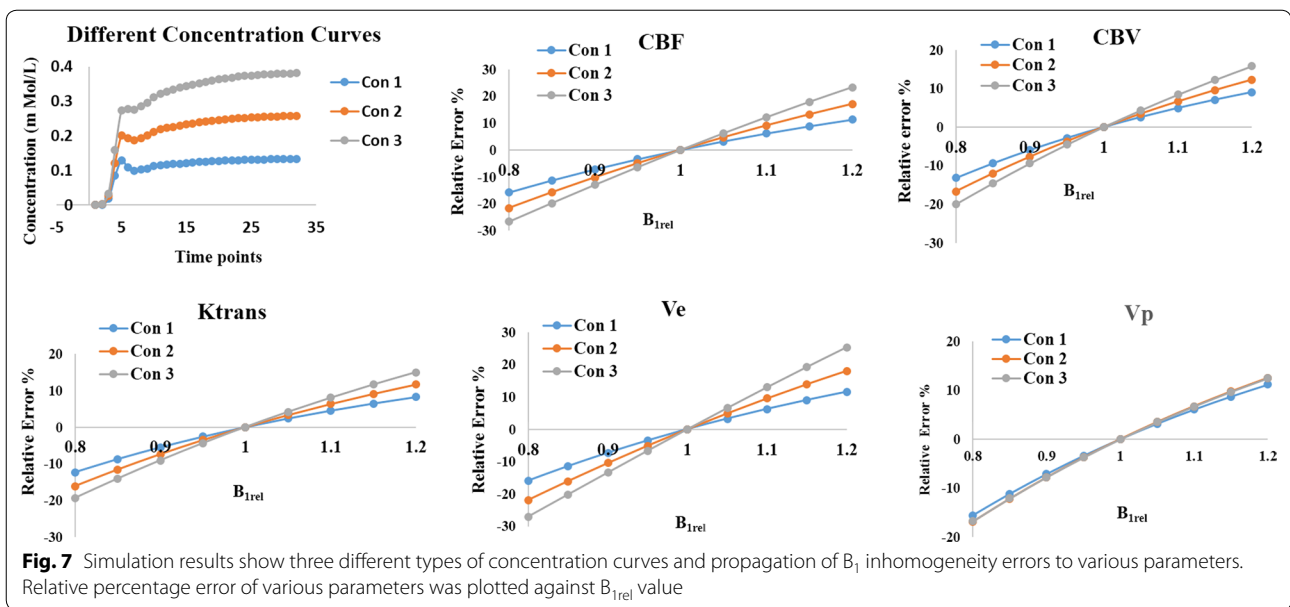
In the current study, lower and upper bound values during T_1 map estimation and Tracer kinetic model fitting using Matlab routines were decided based on physiological constraints of a particular tissue.

The first step in DCE MRI analysis requires pre-contrast T_{10} map calculation. In the current study, T_1 estimation was performed using multi-flip angles. The T1 map obtained was found to be effected by B_1 inhomogeneity. Hence, T_1 map was also corrected for B_1 field inhomogeneity. In the current study, relative percentage error (RPE) of DCE parameters were positive for B_{1rel} values greater than 1 and negative for B_{1rel} values less than 1. This trend is opposite to the findings of Bedair et al. [18]. This is because, in the current study, RPE is calculated with respect to results of post B_1 correction, which is the corrected value.

There is a monotonic increase in RPE of all DCE parameters although not linearly. This is because of the different concentration amount reaching the tumor in each patient and it has been shown in simulation studies that amount of concentration reaching the tumor also plays a role in deciding RPE of perfusion parameters.

It should be mentioned here that 3D acquisition of DCE MRI data can result in inhomogeneous slab selection. However in the current study, tumor from central slice has been chosen in which inhomogeneous slab selection is not a problem.
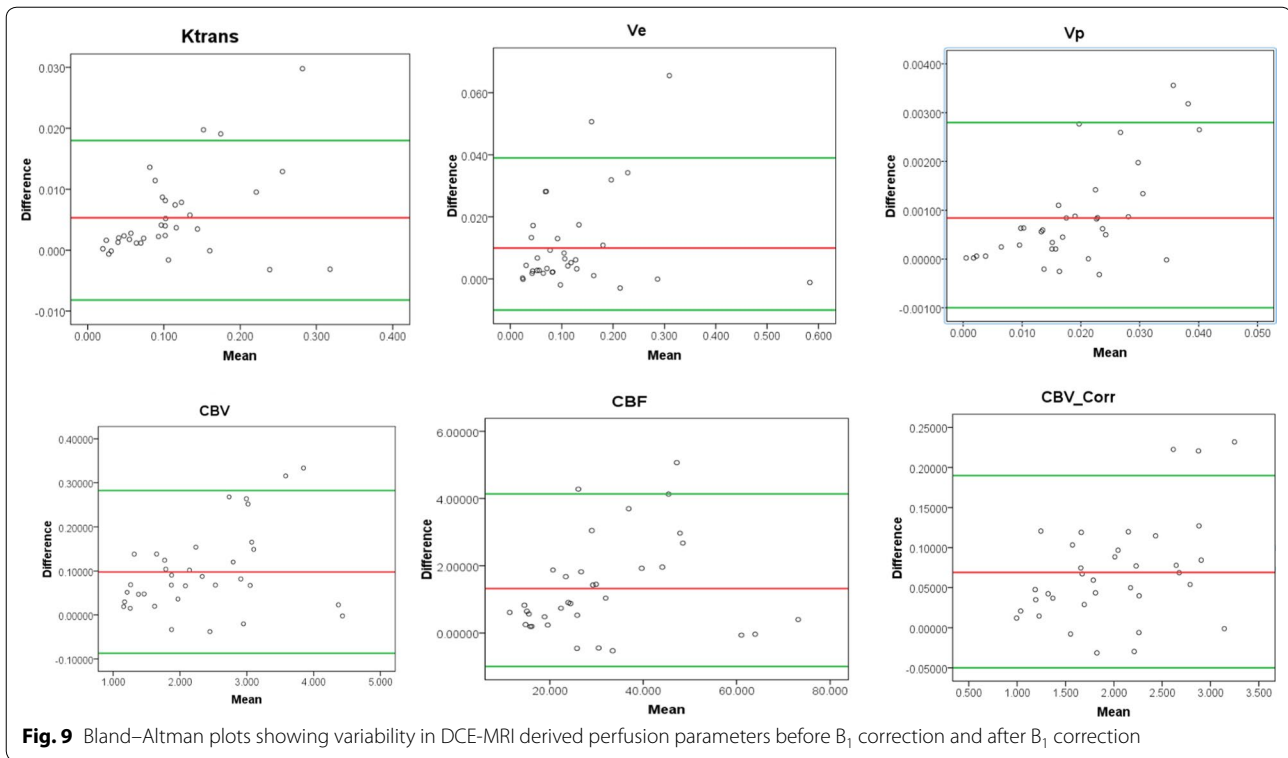
The simulation studies have been designed to evaluate FA related error propagations in a systematic way and to verify the experimental results. Simulation studies helped in covering a wide range of concentration and

Sengupta *et al. J Transl Med* (2017) 15:242

Page 10 of 13

Fig. 7 Simulation results show three different types of concentration curves and propagation of B_1 inhomogeneity errors to various parameters. Relative percentage error of various parameters was plotted against B_{1rel} value

Fig. 8 Simulation results. Scatter plot **a** demonstrates the relationship between errors introduced in B_{1rel} field and that in the kinetic parameter K^{trans} for randomly selected 5 HG and 5 LG patients. Scatter plot **b** the same figure zoomed in at the cut off region

B_1 inhomogeneity, which was difficult to cover using experimental data of the current study. Moreover, experimental data results can be affected by noise, which might influence the true behavior of error propagation. Without simulations, it's difficult to demonstrate that B_1 inhomogeneity errors depend both on B_{1rel} value and initial contrast agent concentration. In the simulation study a $T_1 = 1500$ ms, which is similar to that of enhancing tumor tissue was used to obtain the results. It was found that similar results were obtained for different T_1 values such as 800, 1200 and 2000 ms (results not shown). In the current study, local AIF obtained from each patient data was used for DCE-MRI analysis. However, for simulation studies, global AIF was used. Global AIF can be obtained as an average of local AIFs from different patient data or based on published literature.

It can also be intuitively seen that cut off values for differentiating between grades will be always dependent on tumor location and B_{1rel} value at that ROI. Since, this will be changing from patient to patient, cut off values will also be varying arbitrarily as more and more patients are added to the study. This problem won't arise if B_1 correction is conducted beforehand. Thus the clinical significance of using B_1 correction is intuitively evident.

In a limited in vivo data set, it is not always possible to get appropriate cases where B_1 correction can come into clinical importance. Appropriate cases are those where high B_1 inhomogeneity coincides with ROI (obtained from the maximum CBV_Corr region) within the tumor of glioma patients. This may not happen in many glioma patients and can purely depend on chance depending on tumor ROI location and B_1 inhomogeneity of that ROI.

Sengupta *et al. J Transl Med* (2017) 15:242

Page 11 of 13

Fig. 9 Bland–Altman plots showing variability in DCE-MRI derived perfusion parameters before B_1 correction and after B_1 correction

Thus Bland–Altman plots showed that the mean difference between before and after B_1 corrected perfusion parameters were outside the limits of agreement for few subjects. However, a number of cases were border zone cases. In the current study, the sensitivity, specificity, and AUC of perfusion parameters from ROC analysis did not show much change between pre and post B_1 correction to come to any conclusive decisions (results shown in Additional file 1). Hence, simulations were performed using in vivo data to demonstrate the effect of B_1 inhomogeneity correction on the accuracy of grading. K^{trans} was chosen for simulation studies as it had maximum AUC as was found from ROC analysis (Additional file 1). It needs to be mentioned here that cutoff value of K^{trans} used in simulation studies was from B_1 corrected results. Change in grade has been observed in those cases where the deviation of the value of the grading parameters from cutoff value is less. This suggests that B_1 inhomogeneity may influence glioma grading in cases where perfusion parameter values are on the borderline of cut off value for separating high-grade from low-grade glioma.

It was also observed from Table 3 that for both HG and LG patients, intragroup variation of perfusion parameters reduced after B_1 correction even with a small sample size. This observation highlights the importance of B_1 correction when perfusion parameters are used for clinical diagnosis such as grading.

In this study, the FA used for obtaining DCE-MRI data is 10 degree, which is around two times compared to Ernst angle corresponding to TR of 4.45 ms. The nature of error propagated to DCE-MRI data can also vary depending on the FA used. For a fixed TR, B_1 related errors on dynamic data analysis reduce with increase in FA compared to Ernst angle (observation based on simulation, result not shown). However, this also results in a reduction of SNR in DCE-MRI data. Therefore, a trade-off is usually carried out during protocol designing to select appropriate FA for a fixed TR. On the other hand, B_1 inhomogeneity correction enables to use DCE-MRI data corresponding to FA close to Ernst angle and hence obtain an improved SNR.

One of the limitation is the unavailability of enough patient data so as to illustrate the clinical significance of this study. However, this limitation was addressed by using simulation using in vivo study results. In this study, ROI selection was done on the basis of maximum CBV_Corr values in the tumor region. However, for accurate selection of ROI, those regions should be avoided where high CBV_Corr values coincide with blood vessels. In the current study, we have used SDA based approach for B_1 mapping. There are many alternative sequences which can be used for B_1 mapping. A detailed study needs to be done to investigate how the FA related errors in the quantitative analysis of DCE-MRI data varies with different B_1

Sengupta *et al. J Transl Med* (2017) 15:242

Page 12 of 13

mapping approaches. Another future work in this study is to optimize the FA used for obtaining DCE-MRI data based on B_1 inhomogeneity propagated error.

B_1 field inhomogeneity depends upon MRI scanner field strength, type of coil as well as the type of tissue being studied. A recently reported study on breast DCE-MRI showed an average of 37% FA difference between the right and left breast [18]. B_1 field inhomogeneity increases with increase in MR scanner field strength. For example at 7T, reported studies have shown B_1 field inhomogeneity of $\sim$ 50% in human brain data [33]. Such a large B_1 field inhomogeneity can result in proportional variations in FA, which can lead to errors in DCE-MRI data analysis at 7T. In the current study we have demonstrated results for brain data at 3T; however, similar results should be observed for DCE-MRI studies of different organs as well as at ultra-high field scanner 7T.

Conclusions

In conclusion, a substantial transmit B_1 field inhomogeneity was observed in tumor tissues of the human brain at 3T MRI scanner. It was demonstrated that it can introduce errors in the quantitative parameters derived from DCE-MRI data, which can affect diagnosis and prognosis of patients. B_1 inhomogeneity related errors in the DCE-MRI analysis showed dependence on B_{1rel} values, contrast agent concentration as well as on the length of DCE-MRI data. Overall, B_1 inhomogeneity results in erroneous estimates of quantitative parameters. Correction of FA errors during conversion of S(t) to C(t) can mitigate these errors and provide an improved diagnosis.

Additional file

Additional file 1. ROC analysis of different perfusion parameters before and after B_1 correction.

Abbreviations
B_{1rel}: relative B1; S(t): signal time curve; C(t): concentration time curve; FA: flip angle; RPE: relative percentage error; HG: high grade; LG: low grade.

Authors' contributions
ASe and ASi were involved in protocol/project development, data collection, data analysis and manuscript writing while RKG was involved in protocol/project development, data management, clinical inputs and manuscript editing. All authors read and approved the final manuscript.

Author details
[1] Centre for Biomedical Engineering, IIT Delhi, New Delhi, India. [2] Department of Radiology, Fortis Memorial Research Institute, Gurgaon, India. [3] Department of Biomedical Engineering, AIIMS Delhi, New Delhi, India. [4] Centre for Biomedical Engineering, IIT Delhi, Block-II, Room No. 299, Hauz Khas, New Delhi 110016, India.

Publisher's Note
Springer Nature remains neutral with regard to jurisdictional claims in published maps and institutional affiliations.

References
1. Tofts PS, Kermode AG. Measurement of the blood-brain barrier permeability and leakage space using dynamic MR imaging. 1. Fundamental concepts. Magn Reson Med. 1991;17:357–67.
2. Osaki L, Brasch R, Norman D. Gd-DTPA in clinical MR of lesions. Radiology. 1986;147:1223–30.
3. Aronen HJ, Gazit IE, Louis DN, Buchbinder BR, Pardo FS, Weisskoff RM, et al. Cerebral blood volume maps of gliomas: comparison with tumor grade and histologic findings. Radiology. 1994;191:41–51.
4. Knopp EA, Cha S, Johnson G, Mazumdar A, Golfinos JG, Zagzag D, et al. Glial neoplasms: dynamic contrast-enhanced T2*-weighted MR imaging. Radiology. 1999;211:791–8.
5. Awasthi R, Rathore RKS, Soni P, Sahoo P, Awasthi A, Husain N, et al. Discriminant analysis to classify glioma grading using dynamic contrast-enhanced MRI and immunohistochemical markers. Neuroradiology. 2012;54:205–13.
6. Jung SC, Yeom JA, Kim JH, Ryoo I, Kim SC, Shin H, et al. Glioma: application of histogram analysis of pharmacokinetic parameters from T1-weighted dynamic contrast-enhanced MR imaging to tumor grading. Am J Neuroradiol. 2014;35:1103–10.
7. Tofts PS, Berkowitz B, Schnall MS. Quantitive analysis of dynamic\ mbox{Gd-DTPA} enhancement in breast tumors using a permeability model. Magn Reson Med. 1995;33:564–8.
8. Patlak CS, Blasberg RG. Graphical evaluation of blood-to-brain transfer constants from multiple-time uptake data. Generalizations. J Cereb Blood Flow Metab. 1985;5:584–90.
9. Tofts PS. Modeling tracer kinetics in dynamic Gd-DTPA MR imaging. J Magn Reson Imaging. 1997;7:91–101.
10. Singh A, Rathore RKS, Haris M, Verma SK, Husain N, Gupta RK. Improved bolus arrival time and arterial input function estimation for tracer kinetic analysis in DCE-MRI. J Magn Reson Imaging. 2009;29:166–76.
11. Sahoo P, Rathore RKS, Awasthi R, Roy B, Verma S, Rathore D, et al. Subcompartmentalization of extracellular extravascular space (EES) into permeability and leaky space with local arterial input function (AIF) results in improved discrimination between high- and low-grade glioma

Sengupta *et al. J Transl Med* (2017) 15:242

Page 13 of 13

using dynamic contrast-enhanced (DCE) MRI. J Magn Reson Imaging. 2013;38:677–88.

12. Tofts PS, Brix G, Buckley DL, Evelhoch JL, Henderson E, Knopp MV, et al. Estimating Kinetic parameters from dynamic contrast-enhanced T1-weighted\tMRI of a diffusable tracer: standardized quantities and symbols. J Magn Reson Imaging. 1999;10:223–32.

13. Brix G, Semmler W, Port R, Schad LR, Layer G, Lorenz WJ. Pharmacokinetic parameters in CNS Gd-DTPA enhanced MR imaging. J Comput Assist Tomogr. 1991;15:621–8.

14. Deichmann R. Optimized RF excitation for anatomical brain imaging of the occipital lobe using the 3D MDEFT sequence and a surface transmit coil. Magn Reson Med. 2005;53:1212–6.

15. Singerman RW, Denison TJ, Wen H, Balaban RS. Simulation of B1 field distribution and intrinsic signal-to-noise in cardiac MRI as a function of static magnetic field. J Magn Reson. 1997;125:72–83.

16. Giovanni P, Azlan CA, Ahearn TS, Semple SI, Gilbert FJ, Redpath TW. The accuracy of pharmacokinetic parameter measurement in DCE-MRI of the breast at 3 T. Phys Med Biol. 2010;55:121–32.

17. Azlan CA, Di Giovanni P, Ahearn TS, Semple SIK, Gilbert FJ, Redpath TW. B1 transmission-field inhomogeneity and enhancement ratio errors in dynamic contrast-enhanced MRI (DCE-MRI) of the breast at 3T. J Magn Reson Imaging. 2010;31:234–9.

18. Bedair R, Graves MJ, Patterson AJ, McLean MA, Manavaki R, Wallace T, et al. Effect of radiofrequency transmit field correction on quantitative dynamic contrast-enhanced MR imaging of the breast at 30 T. Radiology. 2015;279:368–77.

19. Gupta SN, Sacolick LI, Hancu I, Tempany-afhdal C, Fennessy FM, Schmidt EJ. Improved T1 mapping and DCE MRI pharmokinetic quantification for prostate at 3T by incorporating B1 inhomogeneity correction. Proc ISMRM'13. 2013;243:151261.

20. Jahng G-H, Stables L, Ebel A, Matson GB, Meyerhoff DJ, Weiner MW, et al. Sensitive and fast T1 mapping based on two inversion recovery images and a reference image. Med Phys. 2005;32:1524–6.

21. Kim SG, Hu X, Uğurbil K. Accurate T1 determination from inversion recovery images: application to human brain at 4 Tesla. Magn. Reson. Med.. Wiley Subscription Services, Inc., A Wiley Company; 1994;31:445–9.

22. Henderson E, McKinnon G, Lee TY, Rutt BK. A fast 3D look-locker method for volumetric T1 mapping. Magn Reson Imaging. 1999;17:1163–71.

23. Messroghli DR, Radjenovic A, Kozerke S, Higgins DM, Sivananthan MU, Ridgway JP. Modified look-locker inversion recovery (MOLLI) for high-resolution T 1 mapping of the heart. Magn Reson Med. 2004;52:141–6.

24. Singh A, Haris M, Rathore D, Purwar A, Sarma M, Bayu G, et al. Quantification of physiological and hemodynamic indices using T1 dynamic contrast-enhanced MRI in intracranial mass lesions. J Magn Reson Imaging. 2007;26:871–80.

25. Fram EK, Herfkens RJ, Johnson GA, Glover GH, Karis JP, Shimakawa A, et al. Rapid calculation of T1 using variable flip angle gradient refocused imaging. Magn Reson Imaging. 1987;5:201–8.

26. Chang LC, Cheng GK, Basser PJ, Pierpaoli C. Linear least-squares method for unbiased estimation of T1 from SPGR signals. Magn Reson Med. 2008;60:496–501.

27. Brookes JA, Redpath TW, Gilbert FJ, Murray AD, Staff RT. Accuracy of T1 measurement in dynamic contrast-enhanced breast MRI using two- and three-dimensional variable flip angle fast low-angle shot. J Magn Reson Imaging. 1999;9:163–71.

28. Cao F, Commowick O, Bannier El, Barillot C. Simultaneous estimation of T1, T2 and B1 maps from relaxometry MR sequences. MICCAI Work. In: Intell Imaging Link. MR Acquis Process. 2014. p. 16–23.

29. Sung K, Daniel BL, Hargreaves BA. Transmit B 1 + field inhomogeneity and T1 estimation errors in breast DCE-MRI at 3 tesla. J Magn Reson Imaging. 2013;38:454–9.

30. Cunningham CH, Pauly JM, Nayak KS. Saturated double-angle method for rapid B1 + mapping. Magn Reson Med. 2006;55:1326–33.

31. Perman WH, Bernstein MA, Sandstrom JC. A method for correctly setting the rf flip angle. Magn Reson Med. 1989;9:16–24.

32. Weiskopf N, Lutti A, Helms G, Novak M, Ashburner J, Hutton C. Unified segmentation based correction of R1 brain maps for RF transmit field inhomogeneities (UNICORT). Neuroimage. 2011;54:2116–24.

33. Singh A, Cai K, Haris M, Hariharan H, Reddy R. On B1 inhomogeneity correction of in vivo human brain glutamate chemical exchange saturation transfer contrast at 7T. Magn Reson Med. 2013;69:818–24.

34. Saekho S, Boada FE, Noll DC, Stenger VA. Small tip angle three-dimensional tailored radiofrequency slab-select pulse for reducedB1 inhomogeneity at 3 T. Magn Reson Med. 2005;53:479–84.

35. Yuan J, Chow SKK, Yeung DKW, Ahuja AT, King AD. Quantitative evaluation of dual-flip-angle T1 mapping on DCE-MRI kinetic parameter estimation in head and neck. Quant Imaging Med Surg. 2012;2:245–53.

36. Pintaske J, Martirosian P, Graf H, Erb G, Lodemann K-P, Claussen CD, et al. Relaxivity of gadopentetate dimeglumine (Magnevist), gadobutrol (Gadovist), and gadobenate dimeglumine (MultiHance) in human blood plasma at 0.2, 1.5, and 3 tesla. Invest Radiol. 2006;41:213–21.

37. Ostergaard L, Smith DF, Vestergaard-Poulsen P, Hansen SB, Gee AD, Gjedde A, et al. Absolute cerebral blood flow and blood volume measured by magnetic resonance imaging bolus tracking: comparison with positron emission tomography values. J Cereb Blood Flow Metab. 1998;18:425–32.

38. Parker GJM, Roberts C, Macdonald A, Buonaccorsi GA, Cheung S, Buckley DL, et al. Experimentally-derived functional form for a population-averaged high-temporal-resolution arterial input function for dynamic contrast-enhanced MRI. Magn Reson Med. 2006;56:993–1000.

39. Sengupta A, Dadarwal R, Gupta R, Singh A. Evaluating effect of B1 field inhomogeneity on DCE-MRI data analysis of brain tumor patients at 3T. Proceedings of the 25th Annual Meeting of ISMRM, HONOLULU, HI, USA, 2017 (Abstract 1430).